Doping-dependent charge injection and band alignment in organic field-effect transistors

B. H. Hamadani,[1] H. Ding,[2] Y. Gao,[2] and D. Natelson[1,3]
[1]*Department of Physics and Astronomy, Rice University, 6100 Main Street, Houston, Texas 77005, USA*
[2]*Department of Physics and Astronomy, University of Rochester, Rochester, New York 14627, USA*
[3]*Department of Electrical and Computer Engineering, Rice University, 6100 Main Street, Houston, Texas 77005, USA*
(Received 5 August 2005; published 2 December 2005)

We have studied metal/organic semiconductor charge injection in poly(3-hexylthiophene) (P3HT) field-effect transistors with Pt and Au electrodes as a function of annealing in a vacuum. At low impurity dopant densities, Au/P3HT contact resistances increase and become nonohmic. In contrast, Pt/P3HT contacts remain ohmic even at far lower doping. Ultraviolet photoemission spectroscopy (UPS) reveals that metal/P3HT band alignment shifts dramatically as samples are dedoped, leading to an increased injection barrier for holes, with a greater shift for Au/P3HT. These results demonstrate that doping can drastically alter band alignment and the charge injection process at metal/organic interfaces.

DOI: 10.1103/PhysRevB.72.235302 PACS number(s): 73.30.+y, 73.61.Jc, 73.61.Ph

Charge injection from metals into disordered organic semiconductors (OSCs) is a complicated physical process for which no complete unified picture exists. Charge transport in disordered OSCs is by hopping through a density of localized states that depends strongly on energy so that the local chemical potential has profound effects on charge mobility.[1,2] Field-effect transistors (FETs) may be used as tools to examine injection by differentiating between the contact resistance, R_c, and the intrinsic channel resistance, R_{ch}. Approaches include analyses of single device characteristics,[3,4] scanning potentiometry,[5–7] gated four-probe measurements,[8] and scaling of total device resistance with channel length in a series of devices.[9–14] Models of injection adapted from inorganic semiconductors have had mixed results. For ohmic injection between Au and P3HT,[11] the contact resistivity is inversely proportional to the intrinsic channel mobility over four decades, over a broad range of temperatures and gate voltages, consistent with diffusion-limited injection.[15,16] However, when a significant barrier Δ exists between the metal Fermi level and the OSC valence band (Cr/P3HT or Cu/P3HT), thermionic emission models cannot explain the field and temperature dependence of the injected current.[7,19] A more sophisticated model[17,18] incorporating a hopping injection into a disordered density of localized states with emphasis on the primary injection event[19,20] explains this nonohmic charge injection data more consistently.

Dopant density strongly influences the magnitude and mechanism of charge injection into OSCs. A doping-dependent charge injection study[22] into P3HT using planar and sandwich geometries has indicated that there are severe contact limitations at low doping densities. Hosseini *et al.* have also shown[21] that contact resistance in disordered OSCs significantly decreases at high doping concentrations due to dopant-induced broadening of the Gaussian density of localized states.

In this paper, we examine doping-dependent charge injection in a series of bottom contact field-effect transistors using Au and Pt as the contacting electrodes and P3HT as the active organic polymer, and find an additional effect of doping. From the length dependence of the total device resistance, R_{on}, we extract the contact and channel resistances as a function of the gate voltage, V_G, and doping. Exposure to air and humidity is known to enhance hole doping in P3HT.[23] As we reduce the concentration of such dopants (related to the bulk P3HT conductivity) by annealing devices in a vacuum at elevated temperatures, R_c and the ratio R_c/R_{ch} increases dramatically for Au/P3HT devices, with injection becoming nonohmic. For Pt/P3HT devices, R_c remains relatively low compared to R_{ch}, and injection remains ohmic even when bulk conductivity is reduced below measurable limits. Ultraviolet photoemission spectroscopy (UPS) reveals that changing dopant concentration strongly alters the band alignment between the metal Fermi level and the OSC valence band. As dopants are removed, the energetic difference between the Au Fermi level and the P3HT valence band increases by about 0.5 eV, while this effect is much less severe in Pt/P3HT. These results demonstrate that doping effects on surface dipole formation, charge transfer at the metal/organic interface, and band bending must be considered in any full treatment of metal/OSC charge injection.

Devices are made in a bottom-contact configuration[11] on a degenerately doped $p+$ silicon wafer used as a gate. The gate dielectric is 200 nm of thermal SiO_2. Source and drain electrodes are patterned using electron beam lithography in the form of an interdigitated set of electrodes with systematic increase in the distance between each pair. The channel width, W, is kept fixed for all devices at 200 μm. The electrodes are deposited by electron beam evaporation of 2.5 nm of Ti and 25 nm of Au or Pt followed by lift off. This thickness of metal is sufficient to guarantee film continuity and good metallic conduction while attempting to minimize disruptions of the surface topography that could adversely affect polymer morphology.

Prior to OSC deposition, the substrates were cleaned for about 2 min in an oxygen plasma. The organic semiconductor, 98% regio-regular P3HT,[24] is dissolved in chloroform at a 0.06% weight concentration, passed through polytetrafluoroethylene (PTFE) 0.2 μm filters and solution cast onto the clean substrate, with the solvent allowed to evaporate in ambient conditions. The resulting films are tens of nanometers thick as determined by atomic force microscopy. The measurements are performed in a vacuum (10^{-6} Torr) in a vari-

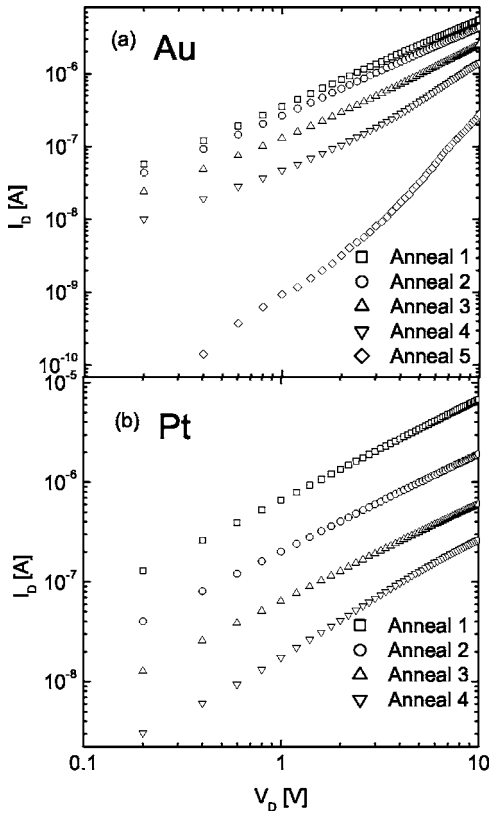

FIG. 1. (a) Log-log plot of the transport characteristics of a Au/P3HT device with $L=10$ μm at $T=300$ K and at a fixed $V_G=-60$ V for different annealing as described in the text. (b) Similar plot for a Pt/P3HT device with identical geometry as (a).

able temperature range probe station using a semiconductor parameter analyzer. To produce a certain doping level, the sample is annealed at elevated temperatures (~350–380 K) in a vacuum for several hours and then cooled down to room temperature for measurement. We characterize the doping by the effective conductivity, calculated from the low V_D source-drain conductance and the estimated P3HT layer thickness at zero gate voltage. In the absence of band bending at the P3HT/SiO_2 interface, there should be no "channel" at the interface, and the measured source-drain conductance should be a bulk effect. We note that similar conductances are found in two-terminal planar devices fabricated on glass substrates. The conductivity after an annealing step remains stable in a vacuum at room temperature and below on the time scale of the measurements, indicating no further change in doping.

The devices operate as standard *p*-type FETs in accumulation mode.[11] With the source electrode grounded, the devices are measured in the shallow channel regime ($V_D < V_G$). Figure 1(a) shows the transport characteristics of a Au/P3HT device with $L=10$ μm at $T=300$ K and at a fixed $V_G=-60$ V for different doping levels. Table I shows the annealing schedule for the Au/P3HT and Pt/P3HT devices. After the fourth annealing step, source-drain transport in the Au/P3HT devices was highly nonlinear. In contrast, Fig. 1(b) shows a similar plot for a Pt/P3HT device with identical parameters as Au above. After a more extensive annealing

TABLE I. Annealing times and temperatures and resulting bulk P3HT conductivities (for average film thickness of 25 nm). For Pt devices bulk conduction following the third and fourth anneals was below detectable limits. A.5* was performed after a few days of air exposure.

	Stage	Time (h)	T (K)	σ (S/m)
Au	anneal A.1	17	350	0.032
	A.2	+7	350	0.022
	A.3	+12	350	0.0077
	A.4	+22	350	8.9×10^{-4}
	A.5*	16	370	
Pt	A.1	24	350	0.064
	A.2	+17	360	0.0036
	A.3	+22	370	
	A.4	+22	380	

process such that bulk P3HT conductivity was reduced below measurable limits, the I_D-V_D data remain nearly linear. To ascertain whether the annealing process irreversibly alters the polymer or the interface, Au/P3HT samples exposed to ambient air were reexamined after several days, and the conductivity had returned to its initial preannealing levels. We carried out an additional annealing stage at this point (A.5*), which reproduced the nonlinearity trend observed earlier.

From the data in Fig. 1, we extracted R_{ch} and R_c from the L dependence of the total device resistance, $R_{on}\equiv\partial V_D/\partial I_D$ as described in Ref. 11. Figure 2(a) shows the V_G dependence of R_c for different annealing steps for the Au device at room temperature. Here we obtain R_c in the limit $|V_D|<1$ V, where transport is still reasonably linear even at higher dedopings. We note that we have developed a procedure for extracting contact current-voltage characteristics even in the limit of strong injection nonlinearities,[19] but it is difficult to quantify such injection by a single number such as R_c. After each anneal, the contact resistance increases significantly. To test for contact-limited transport, we plot the ratio R_c/R_{ch} as a function of V_G for a Au device with $L=10$ μm in Fig. 2(b). At higher dedopings and higher gate voltages, the devices are clearly contact limited. Thus the nonlinear transport seen in this regime at higher biases indicates the possible formation of a charge injection barrier for holes. Analogous data for Pt devices (not shown) reveals that the contact resistance is lower than that observed for Au, and that R_c/R_{ch} remains below 1, only reaching approximately 1 at the most severely dedoped levels.

To further confirm that charge injection from Au electrodes becomes more difficult at lower doping levels than injection from Pt, we fabricated a series of devices (in a two-step lithography process) with *alternating* Au and Pt electrodes. The data are taken twice for each device, once with the source electrode on Au with the drain on Pt and the second time, vice versa. At higher doping levels, the transport data are similar for injection from Au and Pt, but as the sample is annealed, injection from Au becomes more nonlinear and allows for less current at low drain biases. Figure 3

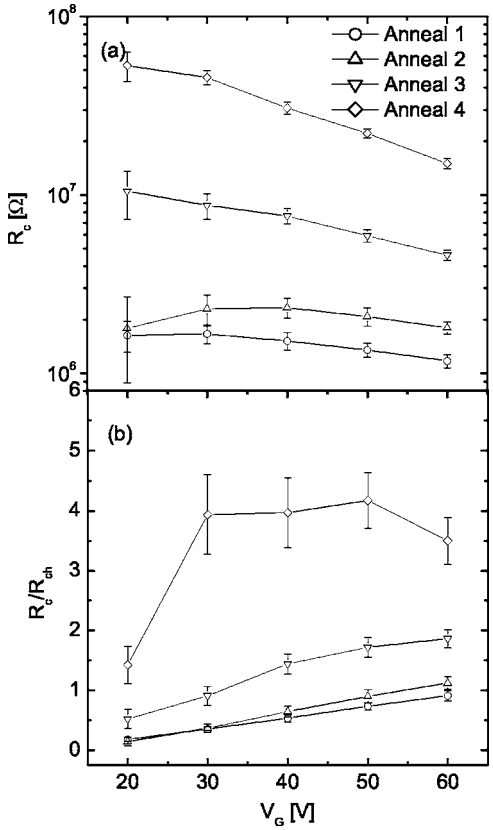

FIG. 2. (a) Gate voltage dependence of R_c for different anneals for the Au device at room temperature. (b) R_c/R_{ch} as a function of V_G for a Au device with $L=10$ μm.

shows a linear plot of I_D-V_D for injection from Au and Pt for a certain dedoped level at $T=300$ K and $V_G=-80$ V with $L=7$ μm and $W=200$ μm. Previous scanning potentiometry experiments[5–7] reveal that in systems with a significant Δ most of the potential drop due to contacts occurs at the source. Figure 3 is consistent with the formation of a larger injection barrier between Au and P3HT than Pt under identical annealing conditions. Note that the lack of nonlinearity in Pt/P3HT/Pt (hole injection from Pt, hole collection by Pt)

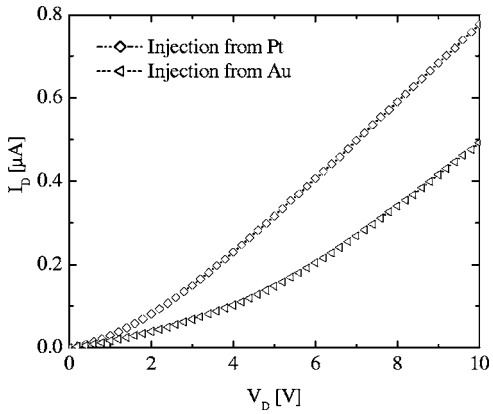

FIG. 3. Linear plot of I_D-V_D for injection from Au and Pt for a sample at 300 K and $V_G=-80$ V. This sample was dedoped such that bulk conductivity at 300 K was below our measurement threshold.

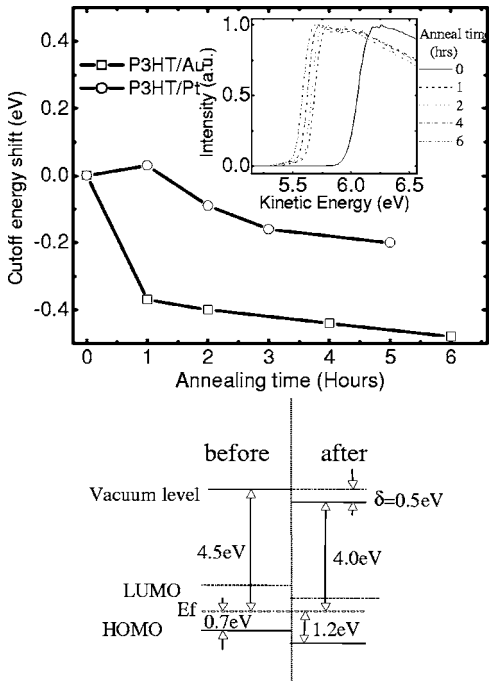

FIG. 4. (a) UPS cutoff energy shift as a function of annealing time for both P3HT/Au and P3HT/Pt. Inset: UPS cutoff of a P3HT/Au sample for different annealing times at 350 K. (b) Energy level diagram of band alignment, based on the results of the UPS data for Au/P3HT before and after the annealing process, showing the large change in the barrier for hole injection.

devices [see Fig. 1(b)] compared with the nonlinear data of Fig. 3 in the Au/P3HT/Pt (hole injection from Au, hole collection by Pt) configuration further supports the conclusion that the *injecting* contact is the source of the nonlinearities.

Dopant concentration clearly affects charge transport across the interface between the OSC and injecting electrodes. Therefore examining the band alignment and interfacial dipole is imperative. Ultraviolet photoelectron spectroscopy (UPS) is a useful tool to monitor changes in the valance electronic structure and the work function of the interface. Previous studies of pentacene-based devices[25] have shown interface dipole formation at the metal/organic interface which varies linearly with the measured metal work function. Here, we show the results of our UPS study for Au/P3HT and Pt/P3HT interfaces. Details of the UPS setup can be found in Ref. 25. Samples were prepared by solution casting of P3HT on thin films (25 nm) of Au or Pt using the same procedures as in the FET devices.

The inset in Fig. 4(a) shows the UPS cutoff of a P3HT/Au sample for different annealing times at 350 K. After 6 h of annealing, the total change in the vacuum level, which appears as a series of shifts in the cutoff data, is about 0.5 eV. The main part of Fig. 4(a) plots the energy shift as a function of annealing time for both Au/P3HT and Pt/P3HT. The cutoff shift for Pt/P3HT after 5 h is 0.2 eV. These shifts correspond to an increase in the Au/P3HT bulk valence level by these amounts. Figure 4(b) shows the band alignment inferred from UPS for Au/P3HT before and after the annealing process. The appearance of 0.5 eV of an additional hole injection barrier is consistent with increased contact resistance

and nonlinear charge injection data shown in Fig. 1(a). Since the energy shift for Pt/P3HT samples is smaller, less contact limitations are expected and observed for these devices. The difference between Au and Pt is likely related to their differing work functions and surface chemistries.

The UPS measurements and energy level diagrams of Fig. 4 do not directly probe the band alignment at the metal/organic interface, since the solution-cast P3HT layer is too thick to permit direct assessment of the metal/P3HT interface. Two effects that are difficult to discriminate in these samples may contribute to the changes in level alignment and injection mechanism with doping: band bending in the bulk, and surface dipole modification directly at the interface.

Band-bending effects have been seen in an experiment[26] involving *p* doping of zinc phthalocyanine, where Gao and Kahn have shown that in addition to the reduction of the interface dipole upon doping, the valence [highest occupied molecular orbital (HOMO)] level shifts towards E_F within a layer thickness of a few nanometers. This shift indicates the formation of a space charge region and band bending near the interface. The improved transport at high doping levels in that experiment is associated with an increase in film conductivity and tunneling of carriers through the now thin interface barrier.

The other possible contribution to the observed change in the injection barrier by annealing is the removal of the interface impurities, most likely H_2O. Heating inside the vacuum can remove H_2O from the metal electrode surface, resulting in more direct contact of the organic with the electrode. The interface barrier in this case will be determined by the metal/organic interface dipole, and it will be smaller for Pt than for Au because of the higher work function of Pt.[25] The smaller barrier for Pt is also supported by the less change of the cutoff upon annealing as observed with UPS. Although the formation of a direct contact to metal will increase the barrier for both Pt and Au, the smaller value of the increase still allows Pt contact to be ohmic. Once reexposed to the ambient, impurities may diffuse back into the interface, resulting in a recovery of the injection properties of the unannealed devices. The reduction of the hole injection barrier by ambient exposure of the metal electrode has recently been observed[27] in another OSC on Au by Wan *et al.*

We note, however, that the annealing processes used in this work are very mild compared to those typically used to remove physisorbed interfacial impurities such as water. Typical UHV baking procedures for desorption require temperatures in excess of 370 K, while we observe significant effects even at 320 K. This suggests that desorption of interfacial impurities is unlikely to be the dominant source of the observed effects.

To examine the physics of charge injection from metals into disordered organic semiconductors, we examined transport properties of a series of organic FETs with P3HT as the active polymer layer and Pt and Au as the source and/or drain electrodes as a function of annealing and resulting dopant concentration. We extract the contact and channel resistances from the length dependence of the resistance, and observed that the contact resistance is dominant and strongly nonlinear at lower dopant concentrations and higher gate voltages for Au/P3HT samples. These effects are much less severe in Pt/P3HT samples. UPS data reveal that upon dedoping, the energy levels shift at the interface, leading to an increased barrier for hole injection. This shift is stronger for Au samples than Pt, consistent with strong nonlinear charge injection observed for Au samples at high dedopings. These results demonstrate that doping can profoundly affect the physics of charge injection in such systems by strongly altering the band alignment between the metal and the organic. The scale of the interface dipole shifts can significantly exceed the dopant-induced broadening of the density of states. Understanding such interfacial charge transfer and band alignment is essential to a complete description of metal/OSC interfaces.

D.N. and B.H. acknowledge partial support by the Research Corporation and the David and Lucille Packard Foundation. D.N. also acknowledges financial support from the Sloan Foundation. H.D. and Y.G. acknowledge support in part by NSF, Contract No. DMR-0305111.

[1] M. C. J. M. Vissenberg and M. Matters, Phys. Rev. B **57**, 12964 (1998).
[2] W. F. Pasveer, J. Cottaar, C. Tanase, R. Coehoorn, P. A. Bobbert, P. W. M. Blom, D. M. de Leeuw, and M. A. J. Michels, Phys. Rev. Lett. **94**, 206601 (2005).
[3] G. Horowitz, R. Hajlaoui, D. Fichou, and A. El Kassmi, J. Appl. Phys. **85**, 3202 (1999).
[4] R. A. Street and A. Salleo, Appl. Phys. Lett. **81**, 2887 (2002).
[5] K. Seshadri and C. D. Frisbie, Appl. Phys. Lett. **78**, 993 (2001).
[6] L. Bürgi, H. Sirringhaus, and R. H. Friend, Appl. Phys. Lett. **80**, 2913 (2002).
[7] L. Bürgi, T. J. Richards, R. H. Friend, and H. Sirringhaus, J. Appl. Phys. **94**, 6129 (2003).
[8] P. V. Pesavento, R. J. Chesterfield, C. R. Newman, and C. D. Frisbie, J. Appl. Phys. **96**, 7312 (2004).
[9] H. Klauk, G. Schmid, W. Radlik, W. Weber, L. Zhou, C. D. Sheraw, J. A. Nichols, and T. N. Jackson, Solid-State Electron. **47**, 297 (2003).
[10] P. V. Necludiov, M. S. Shur, D. J. Gundlach, and T. N. Jackson, Solid-State Electron. **47**, 259 (2003).
[11] B. H. Hamadani and D. Natelson, Appl. Phys. Lett. **84**, 443 (2004).
[12] J. Zaumseil, K. W. Baldwin, and J. A. Rogers, J. Appl. Phys. **93**, 6117 (2003).
[13] E. J. Meijer, G. H. Gelinck, E. van Veenendaal, B. -H. Huisman, D. M. de Leeuw, and T. M. Klapwijk, Appl. Phys. Lett. **82**, 4576 (2003).
[14] G. B. Blanchet, C. R. Fincher, and M. Lefenfeld, Appl. Phys. Lett. **84**, 296 (2004).
[15] J. Campbell Scott and G. G. Malliaras, Chem. Phys. Lett. **299**,

115 (1999).
[16] Y. Shen, M. W. Klein, D. B. Jacobs, J. Campbell Scott, and G. G. Malliaras, Phys. Rev. Lett. **86**, 3867 (2001).
[17] V. I. Arkhipov, E. V. Emelianova, Y. H. Tak, and H. Bässler, J. Appl. Phys. **84**, 848 (1998).
[18] V. I. Arkhipov, U. Wolf, and H. Bässler, Phys. Rev. B **59**, 7514 (1999).
[19] B. H. Hamadani and D. Natelson, J. Appl. Phys. **97**, 064508 (2005).
[20] T. van Woudenbergh, P. W. M. Blom, M. C. J. M. Vissenberg, and J. N. Huiberts, Appl. Phys. Lett. **79**, 1697 (2001).
[21] A. R. Hosseini, M. H. Wong, Y. Shen, and G. G. Malliaras, J. Appl. Phys. **97**, 023705 (2005).
[22] D. B. A. Rep, A. F. Morpurgo, and T. M. Klapwijk, Org. Electron. **4**, 201 (2003).
[23] S. Hoshino, M. Yoshida, S. Uemura, T. Kodzasa, N. Takada, T. Kamata, and K. Yase, J. Appl. Phys. **95**, 5088 (2004).
[24] Sigma-Aldrich Inc., St. Louis, MO.
[25] N. J. Watkins, L. Yan, and Y. Gao, Appl. Phys. Lett. **80**, 4384 (2002).
[26] W. Gau and A. Kahn, Appl. Phys. Lett. **79**, 4040 (2001).
[27] A. Wan, J. Hwang, F. Amy, and A. Kahn, Org. Electron. **6**, 47 (2005).